

A Note on Saturation Ion Currents
to Langmuir Probes

by

Francis F. Chen

MATT-272

June, 1964



PLASMA PHYSICS
LABORATORY

Contract AT(30-1)—1238 with the
US Atomic Energy Commission

PRINCETON UNIVERSITY
PRINCETON, NEW JERSEY

Princeton University
Plasma Physics Laboratory
Princeton, New Jersey

A Note on Saturation Ion Currents
to Langmuir Probes

by

Francis F. Chen

MATT-272

June, 1964

AEC RESEARCH AND DEVELOPMENT REPORT

This work was supported under Contract AT(30-1)-1238 with the Atomic Energy Commission. Reproduction, translation, publication, use and disposal in whole or in part, by or for the United States Government is permitted.

A Note on Saturation Ion Currents
to Langmuir Probes

by

Francis F. Chen
Plasma Physics Laboratory, Princeton University,
Princeton, New Jersey

ABSTRACT

It is shown that the parabolic variation of saturation ion current with probe potential observed in dense plasmas is fortuitous and is unrelated to the effects of orbital motion. Agreement between measured and computed saturation ion characteristics is illustrated. The discussion is in the framework of collisionless, magnetic-field-free theories; they apply to the experiments only if the ion Larmor radius is much larger than the probe radius.

In dense plasmas for which the Debye length h is less than the probe radius r_p , it is often found that the saturation ion flux I_i to a Langmuir probe varies as $(-V_p)^{\frac{1}{2}}$, where V_p is the (negative) probe voltage. This is the dependence expected for cylindrical probes drawing orbital-motion-limited current. In the experiment of Gardner et al.,¹ however, a linear $I_i^2 - V_p$ dependence was observed even though r_p/h was of order 10 and the probe current was almost certainly space charge limited. That such a relationship sometimes holds even for thin sheaths was pointed out by Langmuir² himself; he also pointed out that the erroneous application of the orbital theory to such a case would lead to a spurious value of the space potential.

Gardner et al.¹ conjectured that a linear $I_i^2 - V_p$ relation might come about because the potential at the sheath edge might be proportional to V_p , so that orbital motion limitation might occur in the quasi-neutral region. However, it is more useful to think of the sheath edge potential as being constant and that the radius of the sheath edge increases with probe potential to give the increase in ion current. The reason is that if the absorption radius r_o is defined as the effective collection radius of the probe, or the radius within which all ions are collected, then for a cylindrical probe $\eta(r_o)$ is a universal constant equal to $\ln 2$, where $\eta \equiv -eV/kT_e$. This has been shown recently by Lam³ and previously by Wenzl⁴ for a monoenergetic ion distribution. The result for a

Maxwellian distribution cannot be much different because of the insensitivity of the theory to kT_i .

We now wish to present numerical results which show that the linear dependence of I_i^2 on V_p is fortuitous but is approximately true for certain ranges of parameters. In Figs. 1 and 2 are shown log-log plots of η_p versus dimensionless current J or $J\xi_p$ for spherical and cylindrical probes, respectively, for various values of $\xi_p = r_p/h$. It is seen that J^2 varies approximately as η_p only for large η_p and small ξ_p . These curves were computed by the method of Allen, Boyd, and Reynolds,⁵ which is valid for $\beta \equiv kT_i/kT_e = 0$. For cylinders, this method yields a different result from the $\beta = 0$ limit of a finite- β theory. The reason is that the angular momentum L is assumed to be zero at $r = \infty$ in this theory, while L is finite in the $\beta = 0$ limit of a finite- β theory because of non-uniform convergence.

In Figs. 3 and 4 we show similar curves for $\beta = 0.1$, for spheres and cylinders, respectively. Again one finds that the $J^2 - \eta_p$ relation holds only for certain values of ξ_p and η_p . These curves were computed by the method of Bernstein and Rabinowitz,⁶ which is valid for monoenergetic ion distributions. The variation of these results with β is not great.

In the limit of large ξ_p , that is, of dense plasmas, the shape of the $I_i - V_p$ curve can be expressed in terms of a single universal function by proper scaling of the variables. This result was obtained by Lam³ in a rigorous boundary-layer analysis of the Bernstein-Rabinowitz equations. Results of the theory of Lam are summarized in Figs. 5 and 6, which show normalized I_i^2 as a function of normalized V_p for both cylinders and spheres. Here τ is I_i/I_B , where I_B is the current predicted by Bohm⁷ by neglecting the sheath thickness; and A is essentially a constant but has a weak dependence on β . One sees that the $I_i^2 - V_p$ relation can be approximated by a straight line in all cases except for spherical probes under large voltages. The good fit of the cylindrical probe curve in Fig. 6 to a straight line is entirely accidental; the curve actually has an inflection point in this range of the variables. In terms of normal variables, the equations for the dotted straight lines give the following useful approximate formulas:

$$\text{Sphere:} \quad \frac{d(eI_i)^2}{-dV_p} \frac{\text{amp}^2}{\text{volt}} = 2.6 \times 10^{-20} \frac{Z}{N} \left[n^2 r_p (kT_e)_{\text{eV}} \right]^{2/3}$$

$$\text{Cylinder:} \quad \frac{d(eI_i)^2}{-dV_p} \frac{\text{amp}^2}{\text{volt}} = 3.3 \times 10^{-21} \frac{Z}{N} \left[n^2 r_p (kT_e)_{\text{eV}} \right]^{2/3}$$

$$\text{Cylinder:} \quad \frac{d(eI_i)^2}{-dV_p} \frac{\text{amp}^2}{\text{volt}} = 2.6 \times 10^{-21} \frac{Z}{N} \left[n^2 r_p (kT_e)_{\text{eV}} \right]^{2/3} .$$

Here Z and N are respectively the charge number and atomic weight of the ions, and I_i is the ion flux per cm length in the cylindrical case.

In Figs. 7 and 8 we show the comparison of Lam's theoretical curves with some cylindrical probe measurements made by Kuckes⁸ in a thermally-ionized cesium plasma. Since the magnetic field was about 10 kG in this experiment, the ratio of r_L to r_p was only 3 or 4. In spite of this, it is seen that an excellent fit with theory is obtained for large ξ_p . For $\xi_p \approx 8$ the theory is not expected to be very accurate, and indeed one can discern a difference in slope between theory and experiment in Fig. 7. The value of ξ_p found from the fit with theory yields a value of the plasma density n . In both cases this value was within 18% of that found by ordinary microwave interferometry.

In Fig. 9 we show the data of Gardner et al.,¹ taken from Fig. 8 of Ref. 1. In reducing the data to dimensionless form we have assumed $r_p = 9 \times 10^{-3}$ cm, $l_p = 0.32$ cm, $kT_e = 9$ eV, and $V_s = 30$ v, where l_p is the probe length and V_s the space potential relative to the anode. The ratio r_L/r_p was of order 10^2 in this case. Also shown in Fig. 9 are four points from Kuckes' data of Fig. 7 and theoretical curves from Bernstein and Rabinowitz⁶ (BR) for $\beta = 0.1$ and from Lam³ for $\beta = 1$. The experimental value of β was about 1 in both cases. The theory of Lam is not very accurate for such low values of ξ_p ; on the other hand, BR calculations for $\beta = 1$ are not available. Both theories suffer from the neglect of a spread in ion energies, an effect which should become noticeable at $\beta = 1$.

Although the absolute magnitude of n , about $3 \times 10^{12} \text{ cm}^{-3}$, obtained from the Gardner data is in good agreement with microwave measurements, the slope of the $I_i^2 - V_p$ curve seems to be steeper than theory would predict. This discrepancy cannot be removed by adjustments of the parameters assumed unless the conditions of the experiment were completely different from what one could infer from Ref. 1. For instance, the value of V_s that we took was probably high, but even the drastic assumption $V_s = V_f$ (floating potential), does not remove the discrepancy. Other data given in Ref. 1 give greater disagreement. The very small intercept shown by the data at $\eta_p = 0$ is indicative of a larger sheath-to-probe radius ratio than should have been present. Part of this discrepancy may be due to the neglect of the spread in ion energies, but the agreement between the two sets of theoretical curves shown for different values of β would indicate that the ion distribution probably does not have a great effect.

We are indebted to Dr. A. F. Kuckes for access to his data, to Prof. S. H. Lam for helpful conversations, to Mr. H. Fishman for some of the numerical computations, and to Mr. K. P. Mann for help with the drawings. Further numerically computed ion probe characteristics may be found in another report.⁹

REFERENCES

1. A. L. Gardner, W. L. Barr, R. L. Kelly, and N. L. Oleson, *Phys. Fluids* 5, 794 (1962).
2. I. Langmuir, The Collected Works of Irving Langmuir, ed. by Guy Suits (Pergamon Press, New York, 1961) Vol. 4, p. 64.
3. S. H. Lam, Princeton Univ. Gas Dynamics Laboratory Report 681, AFOSR 64-0353 (1964), Submitted to *Phys. Fluids*.
4. F. Wenzl, *Z. angew. Phys.* 2, 59 (1950).
5. J. E. Allen, R. L. F. Boyd, and P. Reynolds, *Proc. Phys. Soc.* 70B, 297 (1957).
6. I. B. Bernstein and I. Rabinowitz, *Phys. Fluids* 2, 112 (1959).
7. D. Bohm, The Characteristics of Electrical Discharges in Magnetic Fields, ed. by A. Guthrie and R. K. Wakerling (McGraw-Hill Book Co., New York, 1949), p. 45.
8. A. F. Kuckes, Princeton Plasma Physics Laboratory (private communication).
9. F. F. Chen, Princeton Plasma Physics Laboratory Report MATT-252 (1964).

FIGURE CAPTIONS

- Fig. 1. Curves of $\log \eta_p$ vs. $\log J$ for various values of $\xi_p = r_p/h$, for spherical probes and zero ion temperature. Here J is defined by $J = I_i(e^2/kT_e)(m_i/2ZkT_e)^{\frac{1}{2}}$, η_p by $\eta_p = -eV_p/kT_e$, and h by $h^2 = kT_e/4\pi n e^2$.
- Fig. 2. Curves of $\log \eta_p$ vs. $\log J\xi_p$ for various values of ξ_p , for cylindrical probes, zero ion temperature, and zero ion angular momentum. Here $J\xi_p$ is equal to $I_i r_p (e/kT_e)^2 (2m_i kT_e/Z)^{\frac{1}{2}}$, Z being the ion charge number.
- Fig. 3. Curves of $\log J$ vs. $\log \eta_p$ for spherical probes and finite ion energies $E_i = \beta kT_e$. Symbols are as in Fig. 1.
- Fig. 4. Curves of $\log J\xi_p$ vs. $\log \eta_p$ for cylindrical probes and finite ion energies $E_i = \beta kT_e$. Symbols are as in Fig. 2.
- Fig. 5. Curves of τ^2 vs. $A \xi_p^{-4/3} \eta_p$, from the theory of Lam (Ref. 3), which is valid for large ξ_p . For spheres, $\tau \approx I_i / [1.5 \pi r_p^2 n (2ZkT_e/m_i)^{\frac{1}{2}}]$. For cylinders, $\tau \approx I_i / [1.9 r_p n (2ZkT_e/m_i)^{\frac{1}{2}}]$. A range of τ corresponding to relatively thin sheaths is covered.
- Fig. 6. The extension of the curves of Fig. 5 to a range of τ corresponding to thick sheaths.

Fig. 7. Normalized $I_i^2 - V_p$ curves compared with experimental measurements, for a low-density plasma.

Fig. 8. Normalized $I_i^2 - V_p$ curves compared with experiment, for a high-density plasma.

Fig. 9. Normalized $I_i^2 - V_p$ curves compared with the experiments of Gardner et al. (Ref. 1) and of Kuckes (Ref. 8).

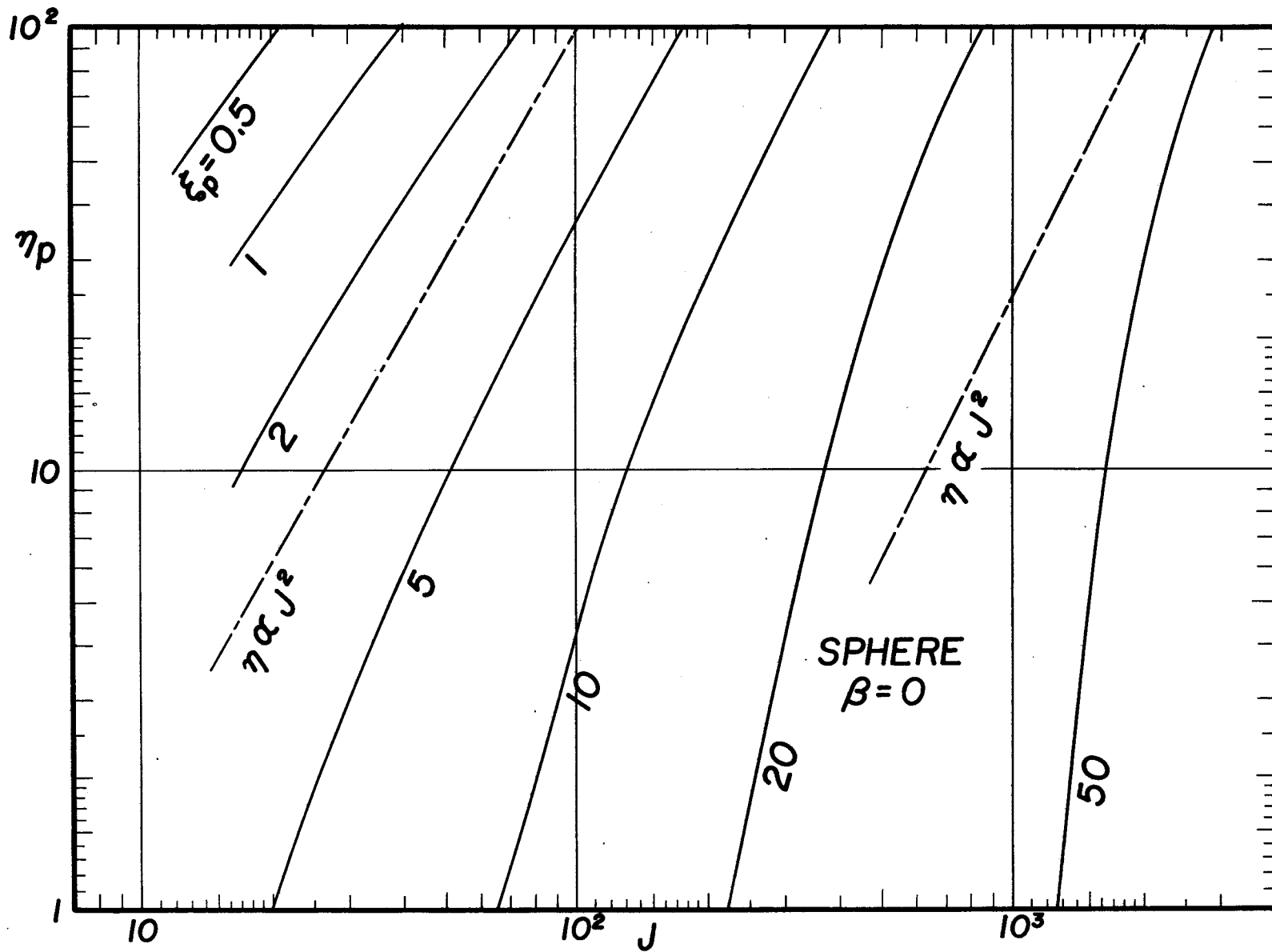
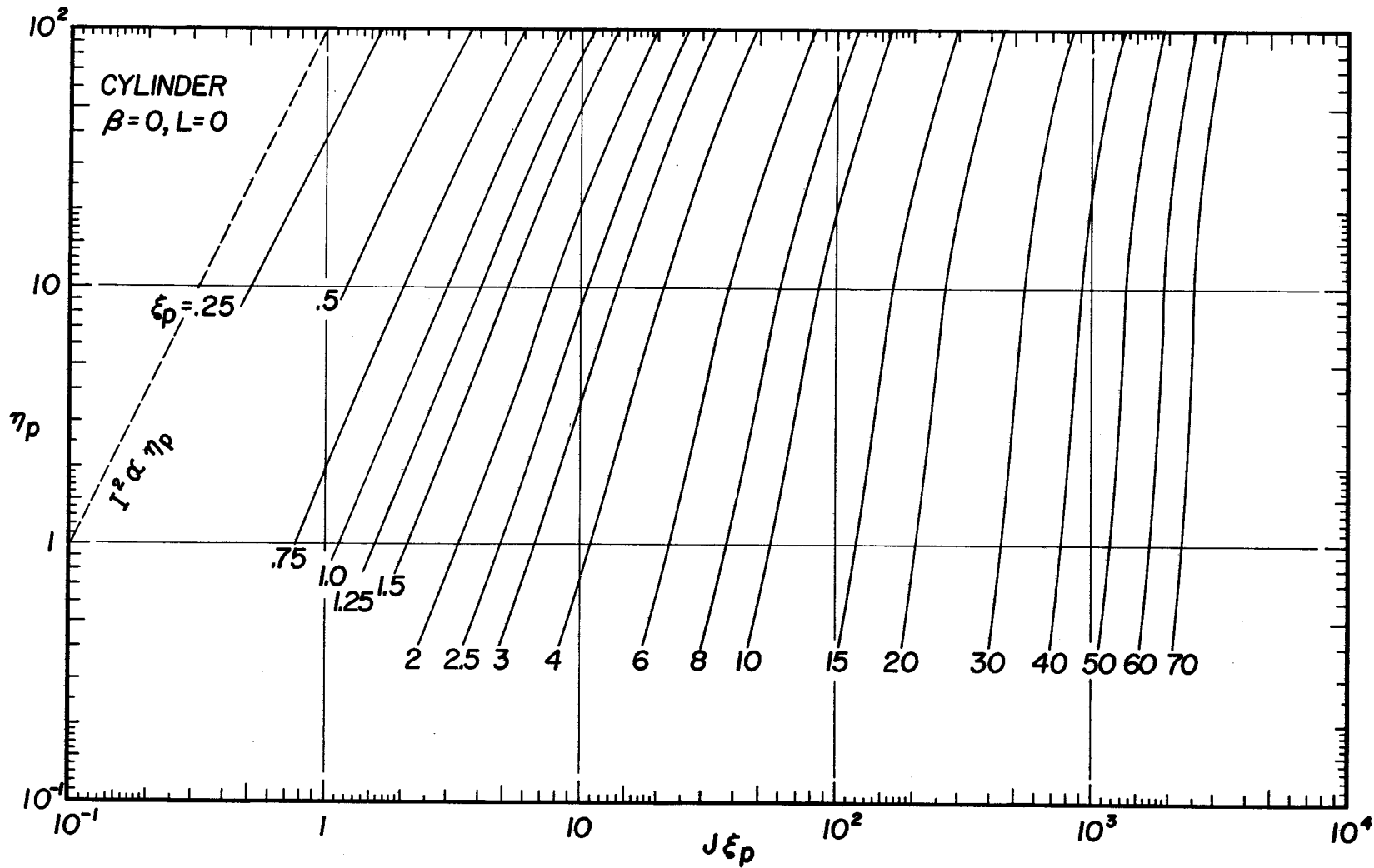
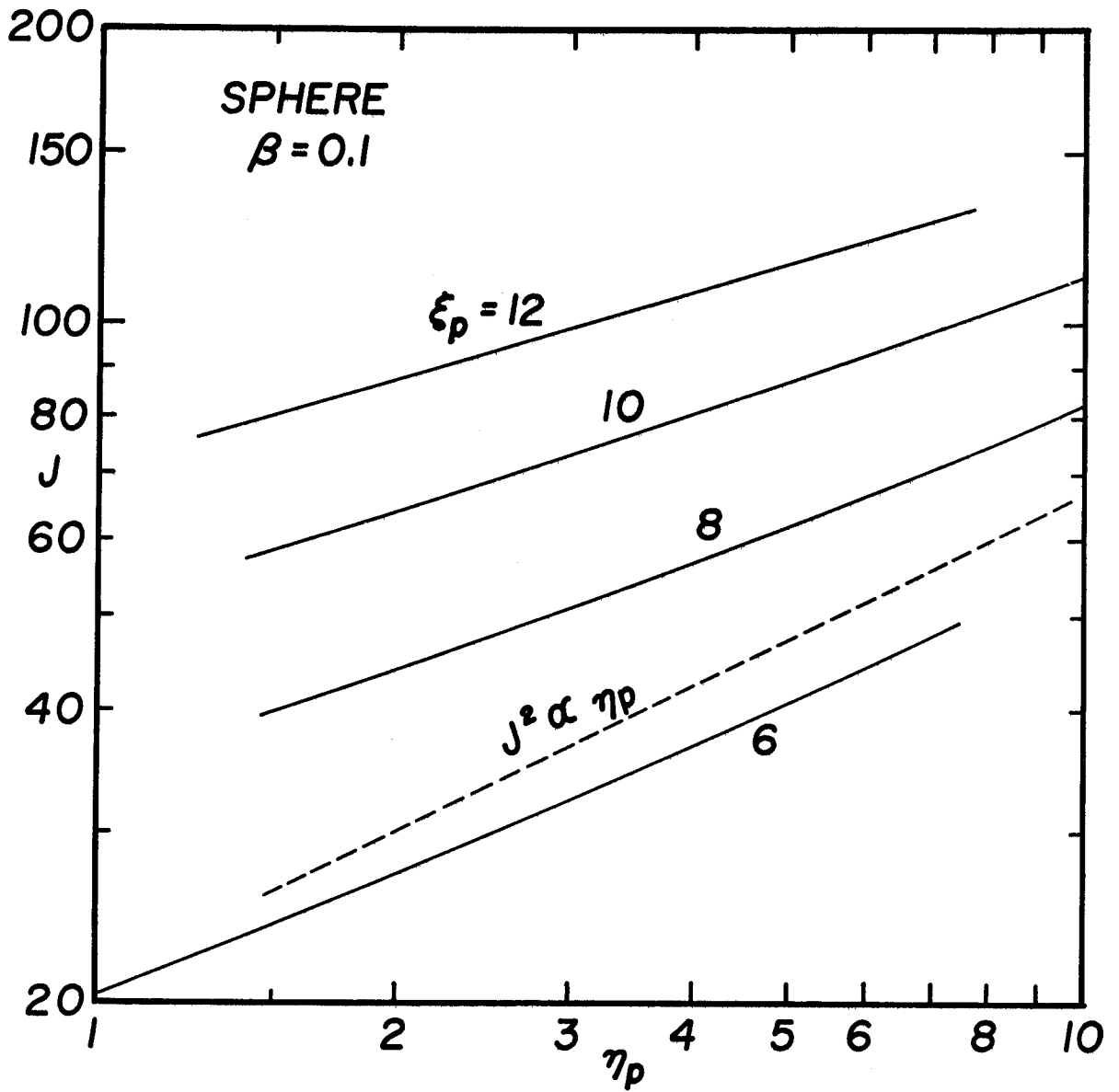


Figure 1



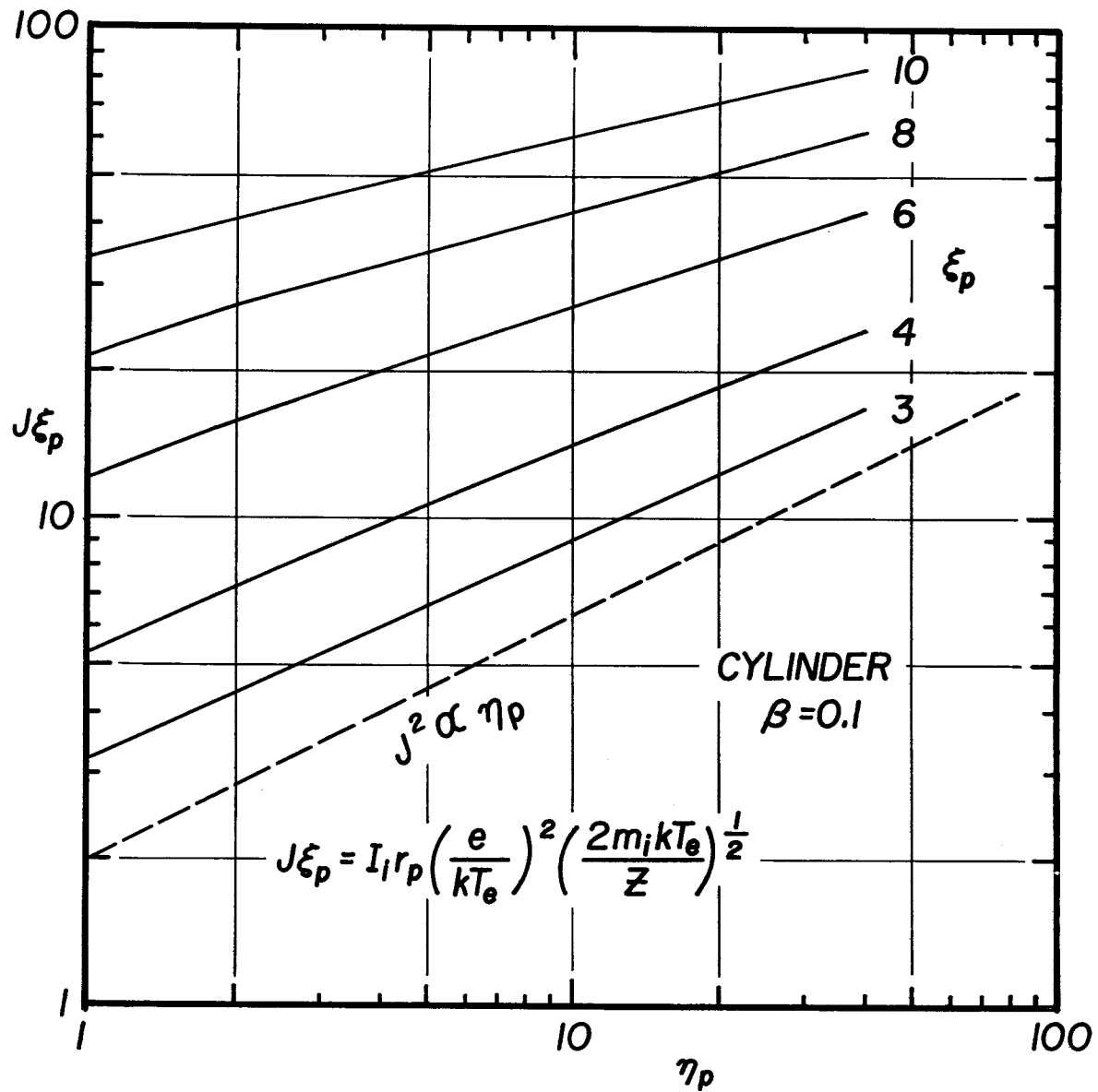
643250

Figure 2



643245

Figure 3



643240

Figure 4

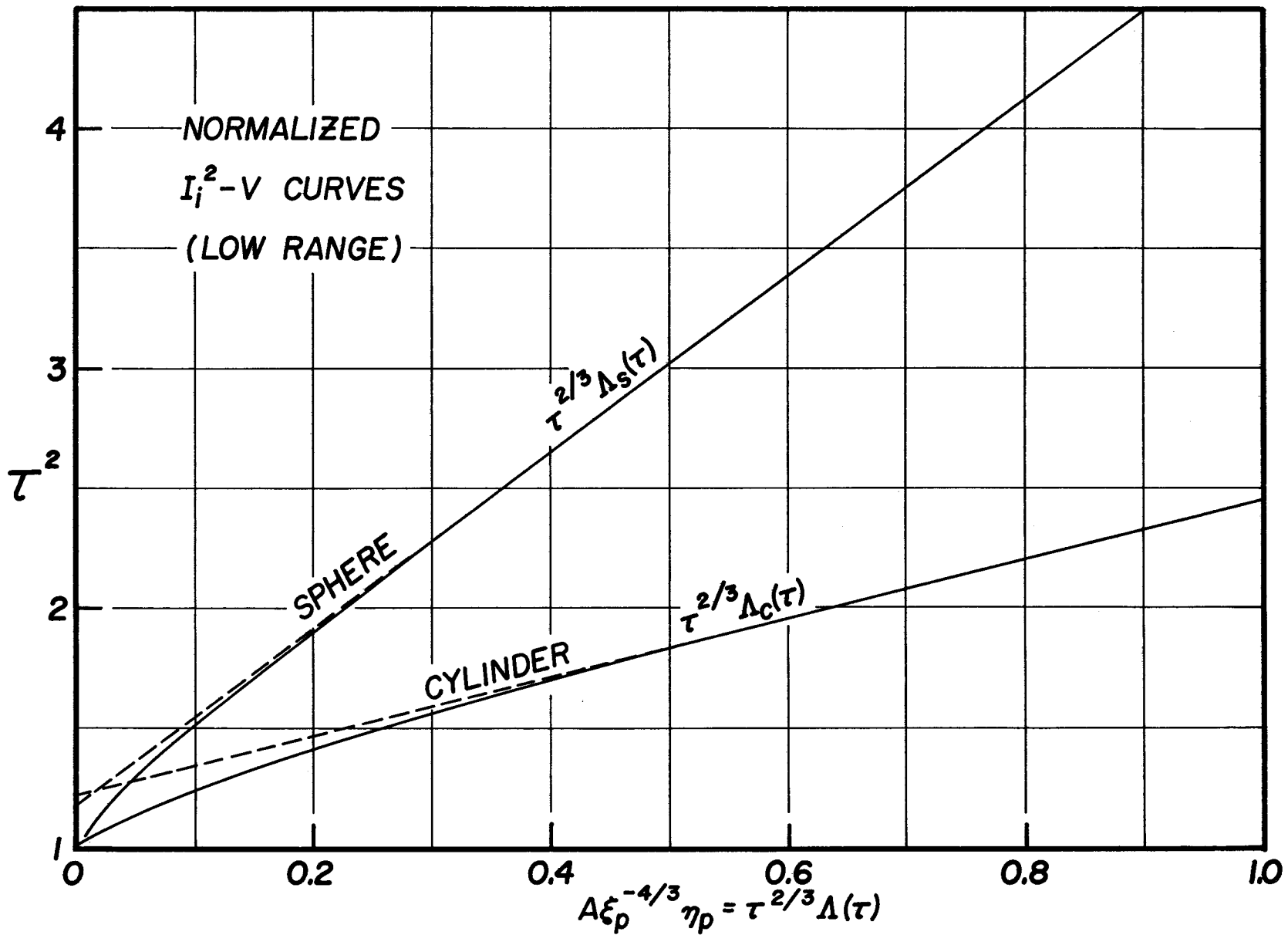
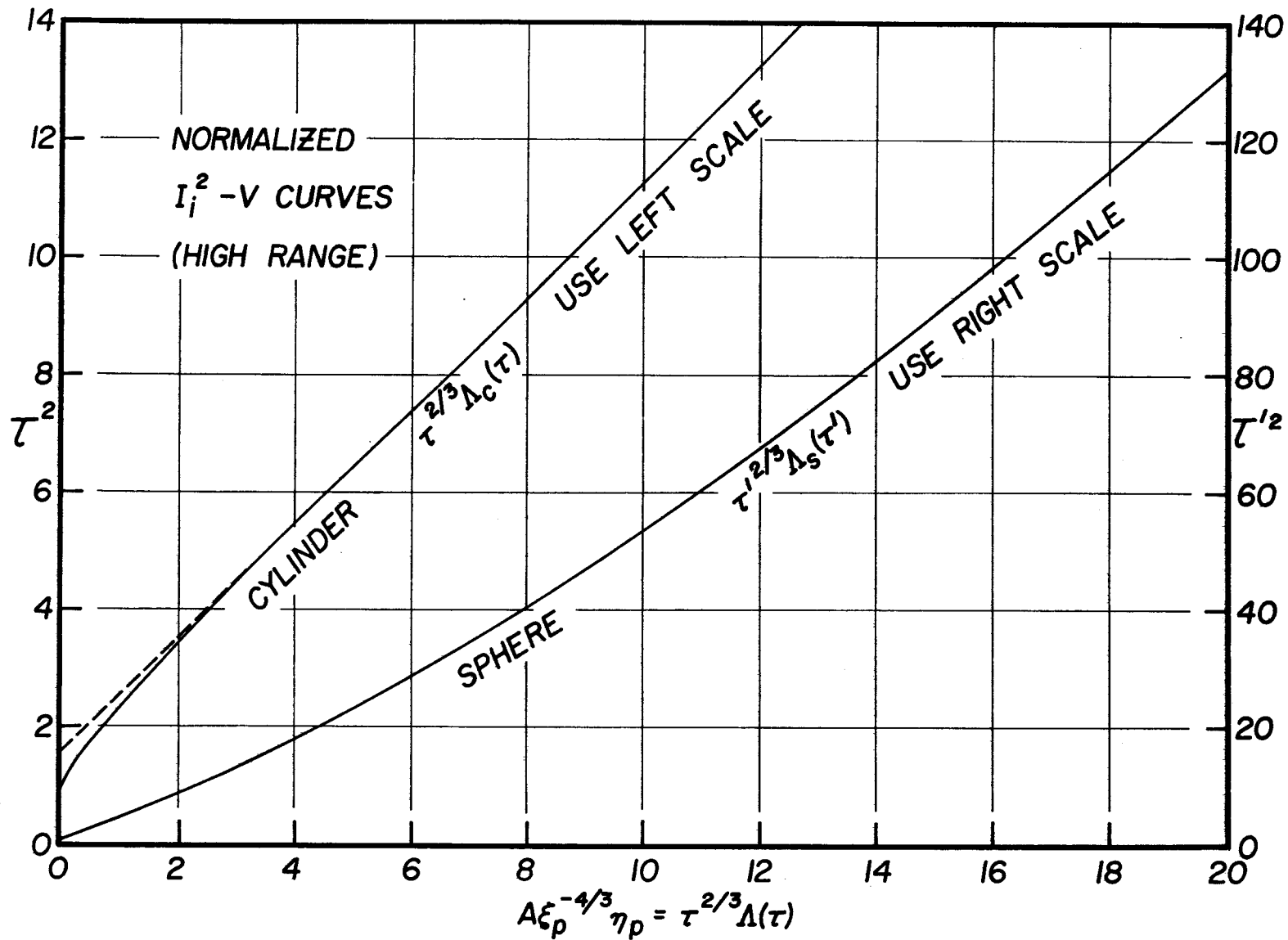


Figure 5



643237

Figure 6

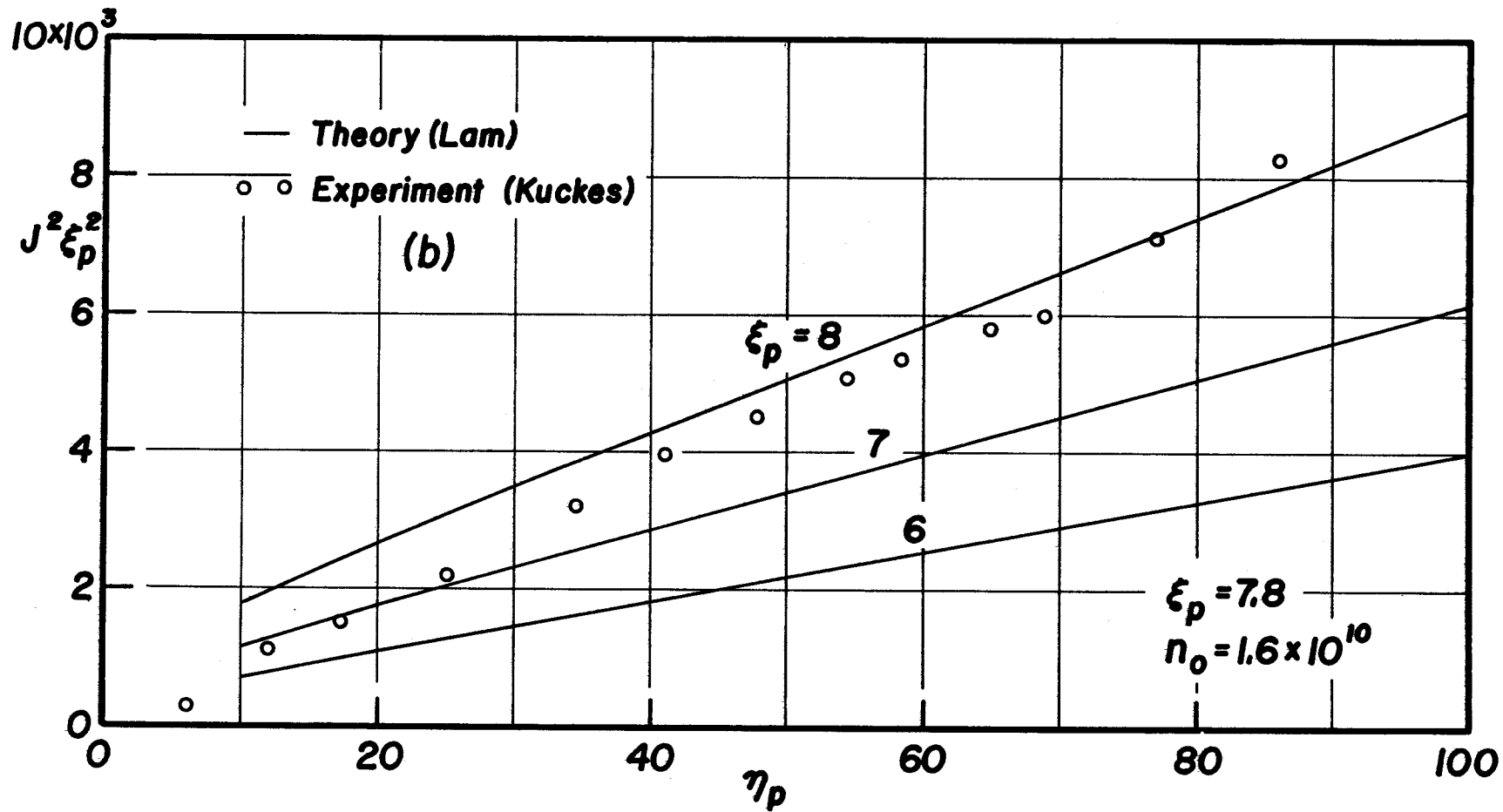


Figure 7

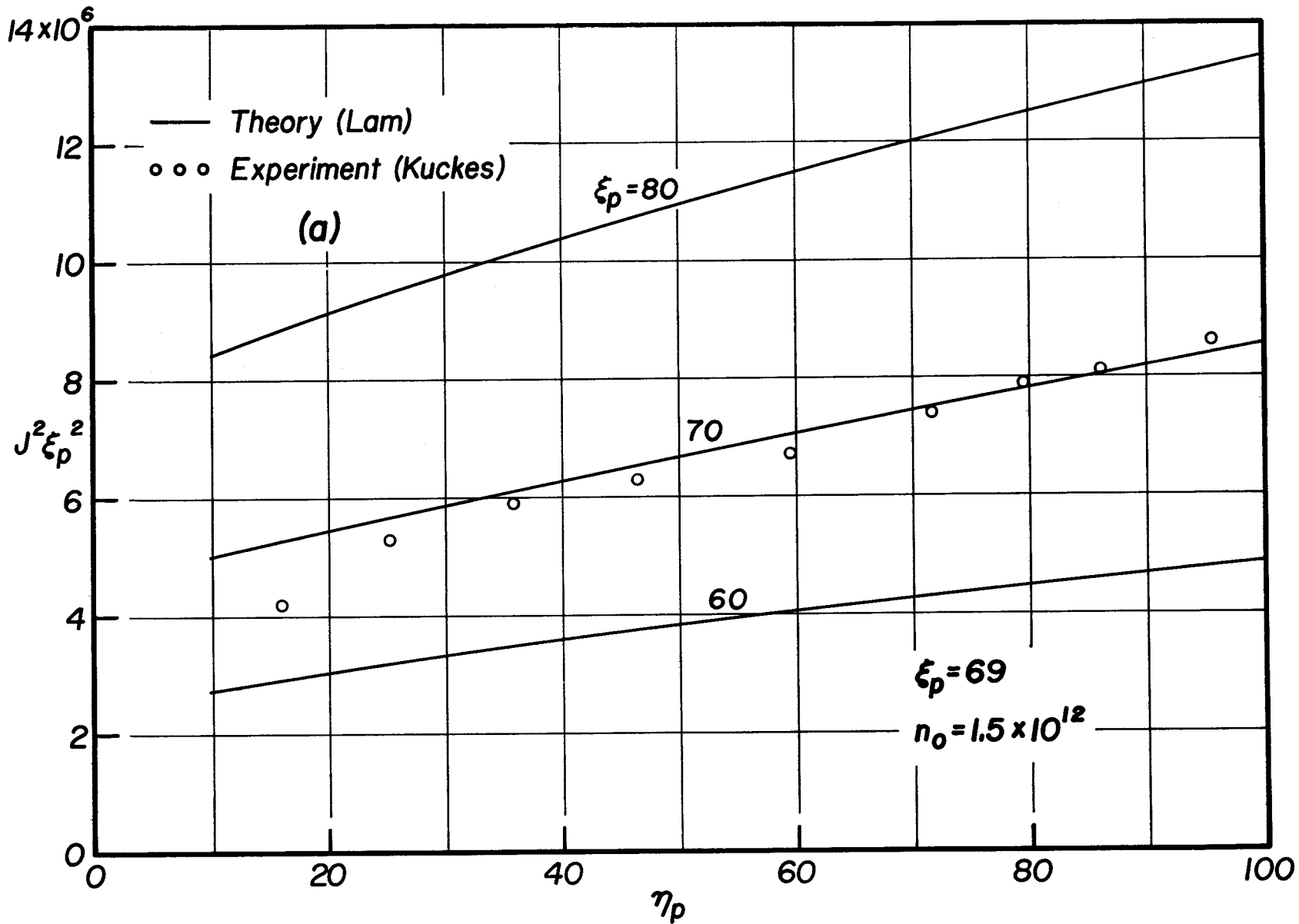


Figure 8

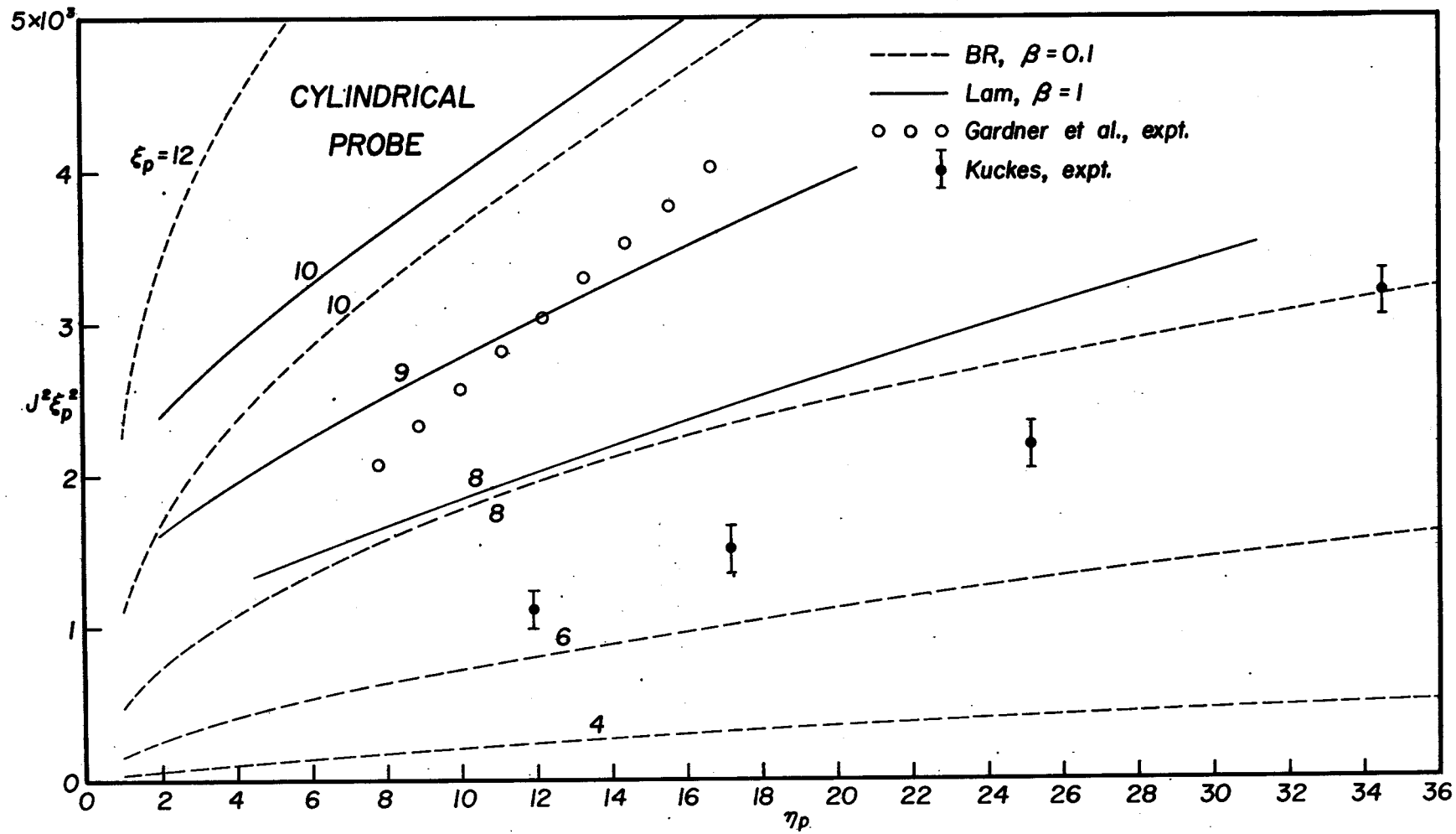


Figure 9